Methodology of quantifying curvature of Fresnel lenses and its effect on CPV module performance

R. Herrero,* C. Domínguez, S. Askins, I. Antón, and G. Sala

Instituto de Energía Solar, Universidad Politécnica de Madrid, Ciudad Universitaria 28040, Madrid, Spain
**rebeca.herrero@ies-def.upm.es*

Abstract: Fresnel lenses used as primary optics in concentrating photovoltaic modules may show warping produced by lens manufacturing or module assembly (*e.g.*, stress during molding or weight load) or due to stress during operation (*e.g.*, mismatch of thermal expansion between different materials). To quantify this problem, a simple method called "checkerboard method" is presented. The proposed method identifies shape errors on the front surface of primary lenses by analyzing the Fresnel reflections. This paper also deals with the quantification of the effects these curvatures have on their optical performance and on the electrical performance of concentrating modules incorporating them. This method can be used to perform quality control of Fresnel lenses in scenarios of high volume production.

OCIS codes: (350.6050) Solar energy; (120.0120) Instrumentation, measurement and metrology; (040 1520) CCD, charge couple device.

References and links

1. P. Benítez, J. C. Miñano, P. Zamora, R. Mohedano, A. Cvetkovic, M. Buljan, J. Chaves, and M. Hernández, "High performance Fresnel-based photovoltaic concentrator," Opt. Express **18**, A25 (2010).
2. L. Wang, P. Su, R. E. Parks, J. M. Sasian, and J. H. Burge, "A low-cost, flexible, high dynamic range test for free-form illumination optics," in International Optical Design Conference and Optical Fabrication and Testing, OSA Technical Digest, p. ITuE3 (2010).
3. P. Su, R. E. Parks, L. Wang, R. P. Angel, and J. H. Burge, "Software configurable optical test system: a computerized reverse Hartmann test," Appl. Opt. **49**, 4404–4412 (2010).
4. Francis A. Jenkins & Harvey E. White, *Fundamentals of Optics* (McGraw-Hill, 1957).
5. A. Cvetkovic, R. Mohedano, O. Gonzalez, P. Zamora, P. Benitez, P. M. Fernandez, A. Ibarreche, M. Hernandez, J. Chaves, and J. C. Miñano, "Performance modeling of Fresnel-based CPV systems: effects of deformations under real operation conditions," AIP Conf. Proc. **1407**, 74–78 (2011).
6. H. P. Annen, L. Fu, R. Leutz, L. González, and J. Mbakop, "Direct comparison of polymethylmetacrylate (PMMA) and silicone-on-glass (SOG) for Fresnel lenses in concentrating photovoltaics (CPV)" Proc. SPIE **8112**, 811204–811204–7 (2011).
7. V. D. Rumyantsev, N. Y. Davidyuk, E. A. Ionova, P. V. Pokrovskiy, N. A. Sadchikov, and V. M. Andreev, "Thermal regimes of Fresnel lenses and cells in "All-Glass" HCPV modules," AIP Conf. Proc. **1277**, 89–92 (2010).
8. T. Schult, M. Neubauer, P. Nitz, and A. Gombert, "Temperature dependence of Fresnel lenses for concentrating photovoltaics," AIP Conf. Proc. **1277**, 85 (2010).
9. T. Hornung, M. Neubauer, A. Gombert, and P. Nitz, "Fresnel lens concentrator with improved thermal behavior," AIP Conf. Proc. **1407**, 66–69 (2011).
10. S. Askins, "Effects of temperature on hybrid lens performance | Browse - AIP Conference Proceedings," AIP Conf. Proc. **1407**, pp. 57–60 (2011).
11. T. Luce and J. Cohen, "The path to volume production for CPV optics," 35th IEEE Photovoltaic Specialists Conference (PVSC) pp. 000487–000492 (2010).
12. R. Leutz, L. Fu, and H. P. Annen, "Stress in large-area optics for solar concentrators" Proc. SPIE **7412,** 741206–741206–7 (2009).
13. R. Herrero et al.,"Concentration photovoltaic optical system irradiance distribution measurements and its effect on multi-junction solar cells " Prog. Photovolt. Res. Appl. **20** 423 – 430 (2012)

14. M. Victoria et al., “Characterization of the spatial distribution of irradiance and spectrum in concentrating photovoltaic systems and their effect on multi-junction solar cells” Prog. Photovolt. Res. Appl. **21** 308 – 318 (2013)
15. C. Domínguez, I. Antón, and G. Sala, "Solar simulator for concentrator photovoltaic systems," Opt. Express **16**, 14894–14901 (2008).
16. R. Herrero, C. Domínguez, S. Askins, I. Antón, and G. Sala, "Luminescence inverse method for CPV optical characterization," Opt. Express **21**, A1028–A1034 (2013).

1. Introduction

Most concentrating photovoltaic (CPV) modules nowadays are based on flat Fresnel lenses as a primary optical element (POE) [1]. These lenses suffer from warping or bending produced during their manufacturing process or after their installation on the module housing. However, there is a lack of knowledge on how to measure these shape errors in a cost-effective way or on how significant their effect is. In this regard, the work presented here becomes a valuable contribution for manufacturers as it gives some guidelines of how to address this matter.

The so-called “checkerboard method” is proposed as a novel approach to promptly evaluate warping in lenses. The method is similar to others focused on specular surfaces like solar concentrators mirrors [2,3], based on the analysis of ray deviations of the reflected light. In particular, the proposed method evaluates Fresnel reflections occurring at the aperture of the lens and quantifies the curvature throughout the lens area. Consequently, the method reveals possible undesirable warping effects.

The causes and magnitude of this shape deformation depend on the lens material, *e.g.*, polymethyl methacrylate (PMMA) or silicone-on-glass (SoG). Furthermore, the impact this lens warping effect has on its optical performance is linked to the particular photovoltaic receiver over which the lens concentrates light. Taking into account these two considerations, the method is applied to several lenses in the paper. After this, the observed lenses deformations are compared with the variations in the electrical performance of a photovoltaic receiver under these lenses at the solar simulator.

2. Description of the method: evaluating lens flatness errors through Fresnel reflections at the lens front surface.

Shape errors in the front surface of flat primary lenses (due to warp or sagging for instance) can be revealed by measuring the Fresnel reflections of incident light that occur at the front surface of the lens. In this regard, a simple setup can be used outdoors to map the sunlight reflected of the primary lenses of a CPV module onto a white Lambertian reflector surface as presented in Fig. 1.

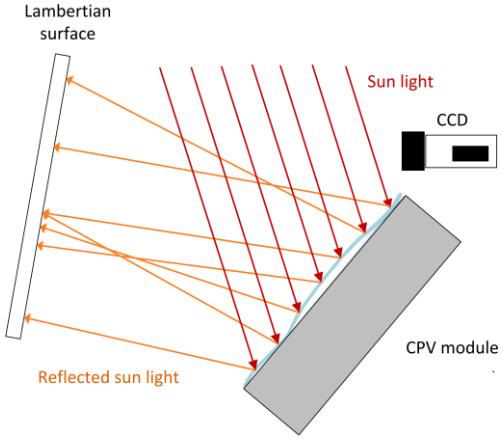

Fig. 1. Set-up used to map the sunlight reflected off the primary lenses of a CPV module onto a white Lambertian surface.

The light map projected on the reflector can be captured using a CCD camera, as presented in Fig. 2 (a). The inhomogeneity in the intensity map is caused by differences in the directions of the Fresnel reflections over the module aperture, which reveals slope fluctuations in the flat side of the lens (waviness). In the case of Fig. 2(a), the CPV module evaluated is formed by 6 optical system-cell units. Each unit has a geometrical concentration ratio of 625X and comprises a single flat Fresnel lens, an inverted refractive pyramid as a secondary optical element (SOE) and a multi-junction (MJ) solar cell (GaInP/GaAs/Ge) as presented in Fig. 2(b). The module has single Fresnel lenses mounted inside slots on side extrusions instead of a parquet.

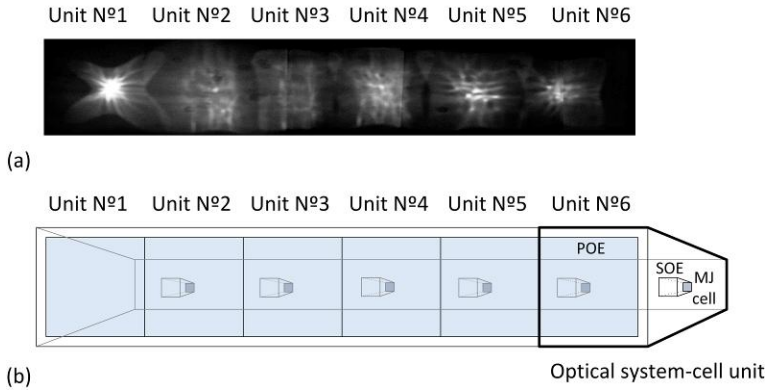

Fig. 2. (a) CCD image showing the Fresnel reflections given in the front surface of a CPV module; (b) The module is formed by 6 optics-cell units (each unit comprises a flat Fresnel lens as primary optical element (POE), an inverted refractive pyramid as a secondary optical element (SOE) and a multi-junction (MJ) solar cell).

A further refinement of this method uses a reference pattern to allow direct quantification of shape errors in lenses. Instead of casting sunlight, the image of a reference pattern (*e.g.*, a checkerboard) reflected on the module aperture (or lens front surface) is captured with a CCD camera. This setup is the basis of the so-called "checkerboard method". It consists in locating the reference pattern in front of the lens or module to be evaluated and then a CCD camera is aimed at the pattern reflection of the lens aperture area. If the front surface of the lens under evaluation is not perfectly flat, the reflected pattern captured by the CCD camera is distorted. This image can then be compared with the one created by a perfectly flat mirror (substituting the Fresnel lens) to assess the existence of form errors and to quantify the shape deformations of the lens.

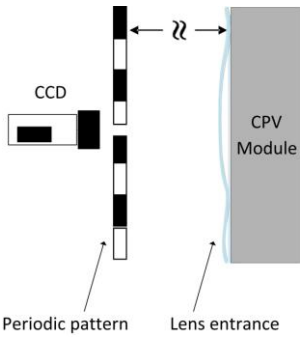

Fig. 3. Set-up of the checkerboard method: the reference pattern is in front of the lens or CPV module to be evaluated and a CCD camera is aimed at the lens aperture area.

The quality of the lens regarding form errors is simply revealed by visual inspection of the reflected checkerboard pattern. For example, in the collection of reflected images

presented in Fig. 4 for the same 6-lens module of Fig. 2(b), lens of unit Nº 1 seems to experiment the largest form errors given that its image is the most distorted.

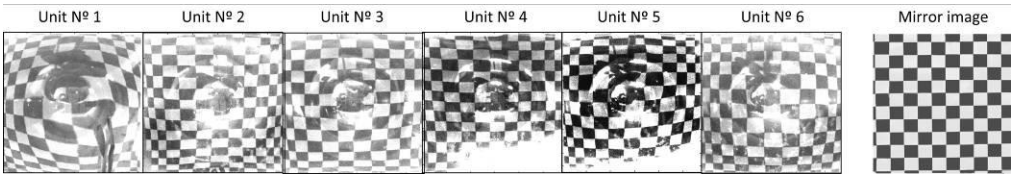

Fig. 4. Images of the Fresnel reflections occurred at the front surface of the 6 lenses (Nº 1 to Nº 6) in the CPV module of Fig. 2(b) versus the Fresnel reflections occurred in a flat mirror (right).

Form errors are quantified through equivalent curvatures: the deformation of the square elements in the captured image (with respect to the reference image) is assumed to be produced by the effect of a quasi-spherical shape of the lens that has a given curvature. The reflected checkerboard pattern of a convex shape becomes smaller, while a concave shape produces a larger pattern. All squares in the reflected pattern suffer the same deformation under paraxial approximation. On the contrary, if the shape of the lens aperture under investigation does not have a constant curvature, the checkerboard pattern is not equally distorted over the entire aperture area of the lens (*i.e.*, squares have different sizes in the image recorded by the CCD camera). In this case, slight differences in curvatures along the lens aperture must be considered.

The lateral magnification of the square elements can be calculated through their size variation with respect to the reference image (flat mirror). The law of reflection for spherical surfaces restricted to images formed by paraxial rays [4] can be used to evaluate the shape (*i.e.*, curvature) that produce such lateral magnification. The expected curvature values associated to long focal distances (longer than 5 meters in most cases) can justify the paraxial approximation. The curvature value is calculated by using the conjugate relations for a spherical mirror provided that both the object distance (*i.e.*, distance from checkerboard to lens/flat mirror) and the object magnification (*i.e.*, size variation of the squares in the checkerboard) are known, and consequently also the image distance (*i.e.*, distance from the lens/flat mirror to the image). In this study, negative and positive curvature values are related to concave and convex shapes respectively.

Software on MATLAB and LabView has been developed to capture the images and calculate the curvatures of lenses as previously described. The developed program processes the CCD images taken by the checkerboard method and calculates the differences in size of the objects in the pattern (*e.g.*, squares) comparing both lens and mirror reflections.

3. Analysis of form errors in Fresnel lenses.

The Fresnel lens is the most popular option for CPV primary optics because is an off-the-shelf and cost effective component in a high volume manufacturing scenario. There are two main technologies for Fresnel lenses production: PMMA lenses manufactured among other techniques by hot-embossing, compression-molding or injection-molding and SoG lenses manufactured by injection-molding or cast-on-glass techniques.

Both PMMA and SoG lenses tend to show deformations produced by quite different causes that can alter the optimum performance of the CPV module [5,6]. However, deformations at the inner surface of the lens are not measurable with the checkerboard method. For SoG, the most critical deformations are caused by the difference in the coefficient of thermal expansion (CTE) between the silicone and the glass, which produces lens facet deformation [7–10] that is not observable with the checkerboard method. Nevertheless, there is a significant bending effect in large SoG lenses, due to the weight of the glass or differential pressures in real operation, that is measurable with the proposed method. In the case of PMMA, it is well known that stress during the manufacturing process may introduce global shape errors, such as warp, because some parts freeze into shape earlier than

others [11,12]. These deformations are measurable by the checkerboard test. Furthermore, temperature variations found in real operation enlarges or shrinks the lens parquet as a whole [6], which may introduce deformations depending on the module housing.

The paper will show, as example case, deformations in PMMA Fresnel lenses and their effect on a CPV module performance. Nevertheless, same methodology can be applied to study the curvature on SoG lenses. Fig. 5 presents some examples of checkerboard-method measurements of representative 25 cm by 25 cm PMMA lenses before installation in a CPV module.

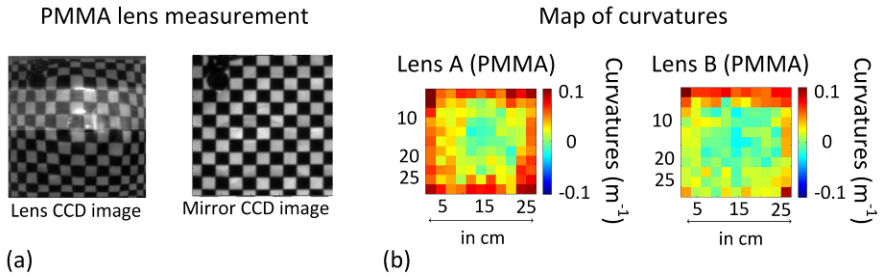

Fig. 5. (a) Examples of CCD images (lens and mirror) with information of the Fresnel reflections in the front surface of lenses made out of PMMA; (b) The maps of curvatures (in m^{-1}) measured by the checkerboard method for two PMMA lenses (lens A and lens B). Negative and positive values are related to concave and convex shapes respectively.

There is an evident surface deformation in the set of unassembled PMMA lenses evaluated in Fig.5. The curvatures values (considering square deformation in both X and Y directions) are within ±0.1 m^{-1} (negative and positive values are related to concave and convex shapes respectively) as presented in Fig. 5(b). In these maps, curvature estimations are performed with a resolution better than cm^{-1}, which basically depends on the area of the lens under evaluation and the pixel resolution of the CCD detector. The spatial sampling resolution of the curvature is directly dependent on the dimensions of the periodic pattern used (2.3 cm in the example of Fig. 5)

Lens curvature can be caused not only by the manufacturing and assembly of lenses but also by degradation in the field. Large shape deformations have been measured in several PMMA samples fielded up to 33 years in different locations (*e.g.*, Riyadh or Phoenix). Both convex and concave shape deformations have been observed for these lens specimens as presented in Fig. 6.

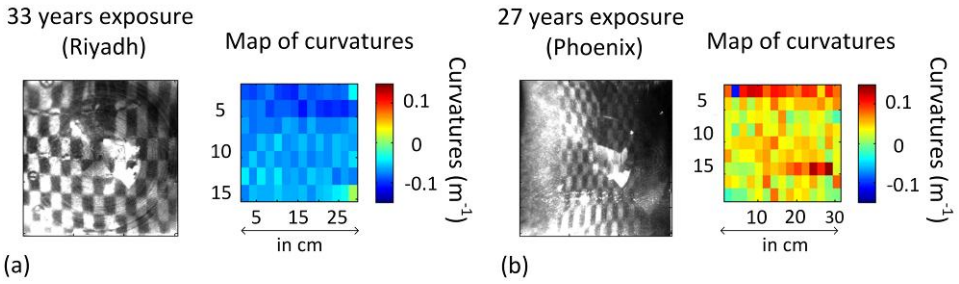

Fig. 6. Examples of CCD images and maps of curvatures (in m^{-1}) measured by the checkerboard method of two Fresnel lenses made out PMMA fielded for several years. Negative and positive values are related to concave and convex shapes respectively.

To define a descriptor for the map of curvatures is highly recommended to relate measured curvatures with the optical performance of the lens. The RMS (Root Mean Square) has been chosen to be the best descriptor of a map of curvatures. It has been found that this figure can be directly related to the optical performance of the lens (presented in section 4).

The effect that curvatures in a lens have in its performance is not only related to their absolute value but also to their signs (convex or concave). Low positive and negative curvatures in a given lens can be more detrimental in the lens performance than only high positive or only high negative values. To take into account the sign of the curvatures, the minimum curvature is subtracted to the map of curvatures before the calculation of the RMS value. The RMS values of the unassembled lenses investigated in this section are presented in the Table 1.

Table 1. RMS of the maps of curvatures for the single and unassembled lenses investigated in section 3

Fresnel lens description	RMS
PMMA lens (A)	0.05
PMMA lens (B)	0.05
PMMA lens (33 years exposure)	0.18
PMMA lens (27 years exposure)	0.04

Form errors in the lens front side have the effect of, among other things, increasing the area of the focused light spot which can be evaluated by means of a CCD camera [13,14]. There are other effects produced by this warping that can only be evaluated by means of a photovoltaic receiver (*i.e.*, solar cell and secondary optical element). Some examples are the variation of optimum focal distance of the lens (related to the maximum power output of the receiver) or the variation of the optical axis of the lens (that produces optical misalignments between the POE and the receiver). The performance of the lens will depend not only on the degree of curvatures but also on the kind of secondary optical element (its size and field of view). In addition, the study of the performance of a single lens without being installed in the module could be not realistic. The misalignments between components during module assembling can be so large that affect the studied lens performance. For that reason, authors believe that is more convenient to connect curvatures and its effect on CPV components by investigating a CPV module.

The next section presents the effects that the form errors in lenses have on the performance of a particular CPV module, with a look at the influence of the module enclosure. The effects of curvatures will depend on the CPV module configuration and characteristics (*e.g.*, number of units, connections in series/parallel, secondary optical element, and concentration ratio among others). Therefore, the section 4 only represents a case of study to show how to implement the methodology of the checkerboard method and how to connect its results to the module electrical performance.

4. Analysis of form errors and their effects in the performance of a CPV module.

The effect of curvature errors in module performance provides the importance of this warp defect. As a case of study, the entrance aperture of a CPV module has been evaluated by the checkerboard method and compared with the electrical characterization of the module (measured at the Helios 3198 CPV solar simulator from Solar Added Value [15]).

The module evaluated, described in section 2, is composed by six individual optical system-cell units connected in series and has been assembled with Fresnel lenses of the same kind than the lenses of Fig 2(b).

4.1. Application of the checkerboard method

The maps of curvatures (in m^{-1}) for the six lenses comprising the module under study are shown in Fig. 7 and their RMS values are presented in the Table 2. From the curvature maps, a tendency to have negative curvatures in the center of the lenses can be observed for the six evaluated samples. However, lens No. 1 has much higher curvature values than the others (the same color map is used for all the units, but the Nº. 1 present curvature values up to -0.18 m^{-1}). These Fresnel lenses share a tendency to show concave deformations in accordance with

the Fresnel lenses before assembling (Fig. 5 (b)), except for lens Nº 1. This indicates that the large warp of this particular lens can be related to the external stress caused by the structure of the module housing or during the mounting process, while the others suffer just a deformation close to the one associated to the lens manufacturing process. Deformations in this particular module are likely due to the fact that lenses are mounted inside slots on side extrusions which can increase the lens deformation if they are not fully parallel.

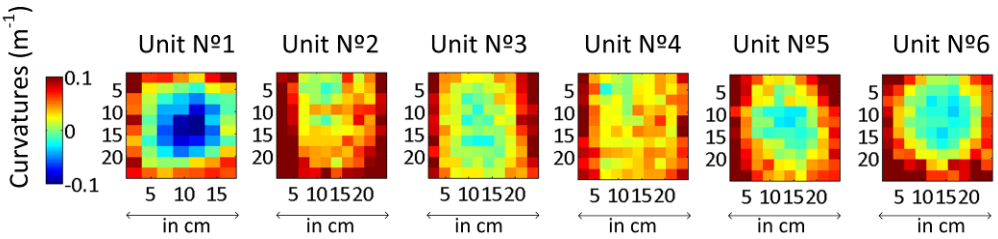

Fig. 7. The maps of curvatures (in m^{-1}) measured by the checkerboard method for the six optical system-cell units presented in the CPV module under study. Negative and positive values are related to concave and convex shapes respectively.

Table 2. RMS of the maps of curvatures for the lenses of the CPV module investigated in section **4**

Position of the Fresnel lens in the CPV module	RMS
Unit Nº 1	0.12
Unit Nº 2	0.07
Unit Nº 3	0.04
Unit Nº 4	0.03
Unit Nº 5	0.04
Unit Nº 6	0.05

4.2. Electrical and optical characterization of the CPV module at the solar simulator: I-V curve and angular transmittance of units.

The I-V curve of the module under study (measured at the solar simulator for CPV) reveals an undesired performance of the concentrator (the output power is approximately 10% lower than expected). The stair-shaped I-V curve in Fig. 8 indicates a mismatch between the currents of the cells, caused by differences in the lens performances since the cells were sorted before installation. At lower voltages, the current of the best performing cells are directed through the bypass diodes of each of the worst performing optical system-cell units. However at near maximum-power-point voltage (V_{MPP}), the worst performing unit limits the module current.

The angular transmittance of each individual optical system-cell unit was measured in the solar simulator by recording the short-circuit current (I_{SC}) corresponding to each cell separately (by masking all units but one at each time and reverse biasing the module to compensate bypass diodes), while modifying the module alignment with respect to the light source [Fig. 9 (a)]. Two parameters are obtained for each unit: the semi acceptance angle ($\pm AA$) or half field of view angle, defined as the angle at which module power reaches 90% of its maximum, and the centroid of the angular transmittance (or pointing vector), calculated as the average value of angles at which the angular transmittance is higher than 90% of its maximum. The misalignments between units are calculated as the differences between their

centroids with respect to a given reference (*e.g.*, the optimum alignment of the module with respect to the light source corresponding to 0 degrees).

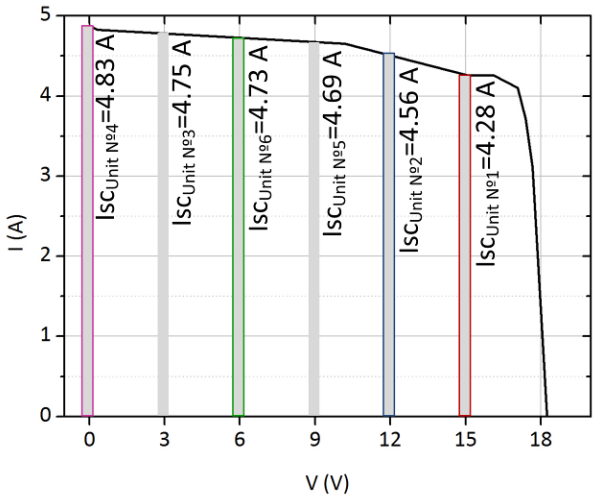

Fig. 8. I-V curve measured for the 6 optical system-cell units presented in the CPV module under study at the Helios 3198 CPV solar simulator (under an irradiance of 850 Wm^{-2}, 25 °C ambient temperature and AM1.5D equivalent spectrum).

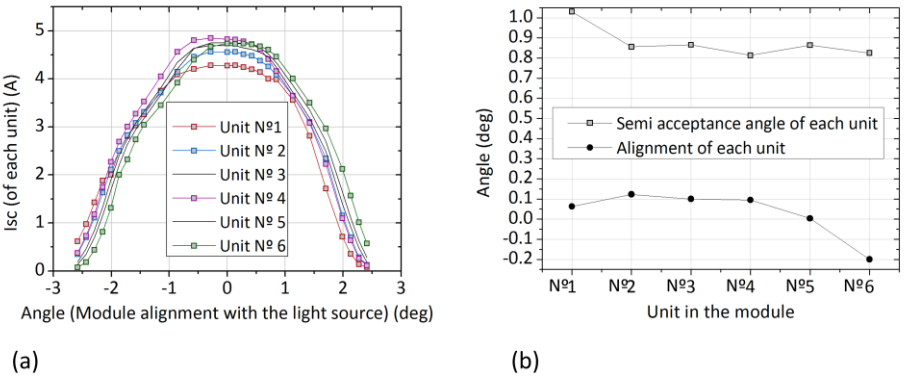

Fig. 9. (a) Measured angular transmittance curves; (b) Misalignments and semi acceptance angle (AA) of the six optical system-cell units of the module under study measured at the Helios 3198 CPV solar simulator (under an irradiance of 850 Wm^{-2}, 25 °C ambient temperature and AM1.5D equivalent spectrum).

4.3. Connecting data obtained by the checkerboard method with the electrical performance of CPV modules

The current mismatch between optical system-cell units in the module may be mainly caused by a varying quality of the receivers and Fresnel lenses, or by an uneven alignment between POE and SOE for all the units. In our example case, the receivers were previously sorted, so we can discard this effect. However, it is difficult to separate the contribution of POE deformations (*e.g.*, warping effect) and pointing errors (caused by a variety of factors as a

wrong positioning of receivers in the back plate) to the observed current mismatch, as both may have similar effects. For example, pointing vector variations can also be caused by deformation of the lens entrance surface.

The angular transmittance curves of the units do not match in shape, but neither in peak value or position (angles range) as presented in Fig. 9(a). In particular, there is a great difference between the photocurrents of unit Nº. 1 and the others [see Fig. 9(a)] and there is a large deviation in the pointing vector of unit 6 [see Fig. 9(b)]. The notably concave shape of the lens Nº. 1 produces light to be focused out of the SOE aperture and thus decreases the photocurrent at the optimum alignment of the unit (*i.e.*, corresponding to the maximum value of the measured angular transmittance). As opposed to this decrease in current there is an increase in the semi acceptance angle, which is obviously artificial inasmuch is associated to a power loss. For the unit Nº. 6, even if is slightly misaligned, its response is still higher than that of unit Nº. 1 because this misalignment is low compared to the acceptance angle of the whole optical system, where the SOE plays an important role. Thus, it can be concluded that the effect of warping identified by the checkerboard method is more critical than the misalignments found between units for this example case. The effect of each map of curvatures on the performance of the CPV module has been quantified and is presented in Fig. 10. The loss of current generated by each cell in the unit has a linear trend with the RMS value of the map of curvatures of the lens in the unit.

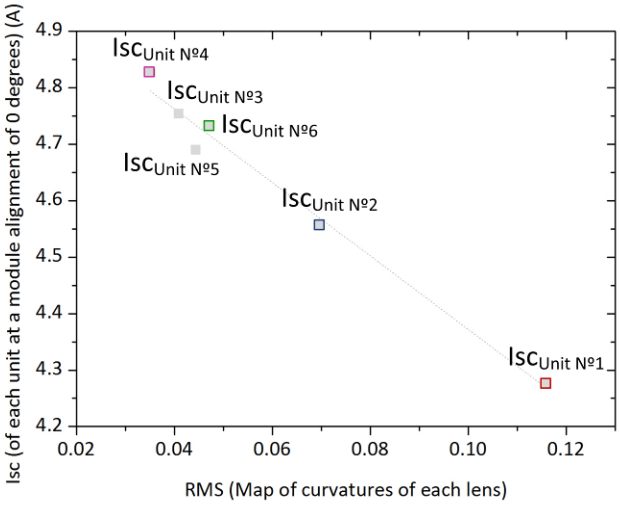

Fig. 10. (a) Current generated by each unit at the module optimum alignment (0 degrees with respect to the light source) in terms of RMS of the maps of curvatures for the lenses of each unit.

Indeed, the CPV solar simulator may provide complete information about the performance of each optical system-cell unit in a CPV module but through a cumbersome process where all units except one are masked at each time. Alternatively, the Luminescence-Inverse method implemented in the sophisticated equipment called Module Optical Analyzer can provide only misalignments between units [16], but it is not able to identify performance losses associated to lens deformation. In this sense, the main advantage of the checkerboard method is its simplicity and high throughput, suitable for the production line of CPV modules, for the identification of lens deformation which can potentially produce significant module performance degradation.

5. Conclusions

Primary lenses in CPV modules suffer internal and external stress that can influence their performance, especially those made of PMMA. For the CPV module studied, lens internal

stress (*e.g.*, molding process of lenses) has been observed to produce curvatures at its entrance surface up to ±0.1 m^{-1}, while external stress (*e.g.*, mounting of lenses in a frame) increases these values up to 0.18 m^{-1}. For the module studied, lens warp has been observed to cause larger power losses than internal misalignments between the components of the module. Long-term outdoor exposure has been also measured to affect warp significantly.

The results from the checkerboard method have been found to be very well correlated with the electrical and optical performance issues actually found through a thorough characterization using a CPV solar simulator. In particular, the RMS of the map of curvature for a given lens has been demonstrated to be closely related to the loss of current experimented for the receiver illuminated with this lens. Thus, this method can be used as a quality control tool at the production line, where a cost-effective tool with a high throughput is required.

Acknowledgments

The research leading to these results has received funding from the European Union Seventh Program FP7/2007-2013 under grant agreement nº 295958 (Project acronym: ECOSOLE), from the Comunidad de Madrid trough the program MADRID-PV-CM (S2013/MAE2780), and from the Spanish Ministerio de Economía y Competitividad (MINECO) under the program I+D –Excelencia 2013 (ENE2013-45299-P) Authors are very grateful to Dr. David Miller and Dr. Hussam Khonkar for the fielded lenses specimens.